

This discussion paper is/has been under review for the journal Biogeosciences (BG).
Please refer to the corresponding final paper in BG if available.

Seasonal distributions and fluxes of ^{210}Pb and ^{210}Po in the Northern South China Sea

C.-L. Wei, M.-C. Yi, S.-Y. Lin, L.-S. Wen, and W.-H. Lee

Institute of Oceanography, National Taiwan University, P.O. Box 23-13, Taipei 106, Taiwan

Received: 29 May 2014 – Accepted: 17 July 2014 – Published: 29 July 2014

Correspondence to: C.-L. Wei (weic@ntu.edu.tw)

Published by Copernicus Publications on behalf of the European Geosciences Union.

BGD
11, 11533–11567, 2014

Discussion Paper | Discussion Paper

Seasonal distributions and fluxes of ^{210}Pb and ^{210}Po in the Northern South China Sea

C.-L. Wei et al.

[Title Page](#)

[Abstract](#)

[Introduction](#)

[Conclusions](#)

[References](#)

[Tables](#)

[Figures](#)

[◀](#)

[▶](#)

[◀](#)

[▶](#)

[Back](#)

[Close](#)

[Full Screen / Esc](#)

[Printer-friendly Version](#)

[Interactive Discussion](#)

Abstract

Vertical distributions of dissolved and particulate ^{210}Pb and ^{210}Po in the water column at the SouthEast Asian Time-series Study (SEATS, $18^{\circ}00' \text{N}$ and $116^{\circ}00' \text{E}$) station in the northern South China Sea were determined from 4 cruises between January 2007 and June 2008. A large deficiency of ^{210}Pb , $379 \pm 43 \times 10^3 \text{ dpm m}^{-2}$, from the secular equilibrium was found within the 3500 m water column. On the other hand, a smaller deficiency of ^{210}Po , $100 \pm 21 \times 10^3 \text{ dpm m}^{-2}$, relative to ^{210}Pb was found in the water column. Time-series data showed insignificant temporal variability of the ^{210}Pb and ^{210}Po profiles. To balance these deficiencies, the removal fluxes for ^{210}Pb and ^{210}Po via particle settling range from 45 to $51 \text{ dpm m}^{-2} \text{ d}^{-1}$ and from 481 to $567 \text{ dpm m}^{-2} \text{ d}^{-1}$, respectively, are expected at 3500 m. The ^{210}Pb removal flux is comparable with, whereas the ^{210}Po removal flux is much higher than, the flux directly measured by moored sediment traps. The discrepancy between the modeled ^{210}Po flux and the measured flux suggests that sporadic events that enhance ^{210}Po removal via sinking ballast may occur in the water column at the site.

1 Introduction

Within the context of carbon sequestration and elemental cycling, material conveyance through particle settling from the surface layer to the deep ocean is an important pathway of elemental removal in the ocean. In view of the important role played by particulate matter, information obtained from the temporal and spatial distributions of particle-reactive radionuclides can provide insight into particle dynamics in the ocean (Cochran and Masque, 2003). The distributions of ^{210}Pb ($t_{1/2} = 22.3 \text{ yr}$) and ^{210}Po ($t_{1/2} = 138 \text{ d}$) have been used extensively by marine chemists to determine the removal rates of particles and associated elements from the ocean (Bacon et al., 1976; Nozaki et al., 1990). Although both ^{210}Pb and ^{210}Po are particle-reactive, there exist subtle differences in the geochemical behaviour of the two radionuclides in the ocean. For example, ^{210}Pb

BGD

11, 11533–11567, 2014

Discussion Paper | Discussion Paper

Seasonal distributions and fluxes of ^{210}Pb and ^{210}Po in the Northern South China Sea

C.-L. Wei et al.

[Title Page](#)

[Abstract](#)

[Introduction](#)

[Conclusions](#)

[References](#)

[Tables](#)

[Figures](#)

◀

▶

◀

▶

[Back](#)

[Close](#)

[Full Screen / Esc](#)

[Printer-friendly Version](#)

[Interactive Discussion](#)



Seasonal
distributions and
fluxes of ^{210}Pb and
 ^{210}Po in the Northern
South China Sea

C.-L. Wei et al.

[Title Page](#)

[Abstract](#)

[Introduction](#)

[Conclusions](#)

[References](#)

[Tables](#)

[Figures](#)

[◀](#)

[▶](#)

[◀](#)

[▶](#)

[Back](#)

[Close](#)

[Full Screen / Esc](#)

[Printer-friendly Version](#)

[Interactive Discussion](#)



tends to be scavenged by inorganic particles, whereas polonium has a higher affinity to biogenic particles (Cherry et al., 1975; Fisher et al., 1988), which results in a shorter residence time of ^{210}Po compared to ^{210}Pb in the surface ocean (Bacon et al., 1976). In addition, atmospheric input via aerosol deposition is the dominant source for ^{210}Pb in the upper layer of the ocean, whereas an atmospheric source is almost negligible for ^{210}Po (Turekian et al., 1977).

Known as a semienclosed marginal sea, the South China Sea is an oligotrophic system under the influence of monsoonal modulation (Tseng et al., 2005). Besides sparse data in the surface water (Nozaki et al., 1998; Wei et al., 2015; Yang et al., 2006), vertical profiles of ^{210}Pb and ^{210}Po in the South China Sea have been reported by Obata et al. (2004) and Chung and Wu (2005). Obata et al. (2004) measured ^{210}Pb and ^{210}Po activities in unfiltered seawater, whereas Chung and Wu (2005) measured dissolved and particulate ^{210}Pb and ^{210}Po . When a comparison is made, it is surprising to note that a large difference exists between the two data sets. Not only systematic discrepancies of ^{210}Pb and ^{210}Po concentrations, but also large differences of the degrees of disequilibria of $^{210}\text{Pb}/^{226}\text{Ra}$ and $^{210}\text{Po}/^{210}\text{Pb}$ were found between the two studies. Obata et al. (2004) found the deviation of ^{210}Po from secular equilibrium in the whole water column to be small. On the contrary, a large deficiency of ^{210}Po relative to ^{210}Pb was reported by Chung and Wu (2005) and led to their conclusion that ^{210}Po is removed in an unorthodox way quickly by picoplankton uptake then transferred to the higher trophic level in the northern South China Sea. In order to determine the correct geochemical processes controlling the behavior of ^{210}Pb and ^{210}Po , it is necessary to verify the distributions of ^{210}Pb and ^{210}Po in the South China Sea.

In a previous paper, Wei et al. (2011) used ^{234}Th , ^{210}Pb , and ^{210}Po data in the upper 200 m to estimate the export fluxes of carbon from the euphotic layer of the SEATS time-series station. Here we emphasize the ^{210}Pb and ^{210}Po geochemistry in the deep basin of the South China Sea. In addition to water column data, sinking fluxes of ^{210}Pb and ^{210}Po in the deep basin were determined by data from sediment traps. The goals of this study are: (1) to resolve the discrepancy between vertical distributions

of ^{210}Pb and ^{210}Po between the two studies by Obata et al. (2004) and Chung and Wu (2005), (2) to compare the geochemical behavior of ^{210}Pb and ^{210}Po , (3) to investigate seasonal variations of the scavenging process, and (4) to compare the trap-measured fluxes of ^{210}Pb and ^{210}Po estimated from $^{210}\text{Pb}/^{226}\text{Ra}$ and $^{210}\text{Po}/^{210}\text{Pb}$ disequilibria, respectively, in the water column of the northern South China Sea.

2 Materials and methods

2.1 Seawater

Seawater samples were collected from four cruises to SEATS (Fig. 1), onboard the R/V *Ocean Researcher I* (ORI-821: 12–19 January 2007, ORI-845: 21–30 October 2007,

10 ORI-866: 28 May–3 June 2008) and R/V *Ocean Researcher III* (ORIII-1239: 28 July–3 August 2007). A CTD/20 L Go-Flo system was used to collect large volumes of seawater for ^{210}Pb and ^{210}Po determinations. At each sampling depth, 20 L seawater was collected and divided into two 10 L subsamples to determine ^{210}Pb and ^{210}Po , respectively. Seawater was immediately pressure-filtered with compressed air through a pre-
15 weighed 142 mm Nuclepore filter (0.45 μm) mounted in a Plexiglas filter holder. The analytical procedures described in Wei et al. (2009) were followed. In short, the filtrate from the ^{210}Po sample was acidified with about 10 mL concentrated HCl and spiked with 2.2 dpm of ^{209}Po and 30 mg of Fe carrier. Given 2 days' isotopic equilibration time, concentrated NH_4OH was then added to raise the pH to approximately 8 to precipitate
20 $\text{Fe}(\text{OH})_3$. The $\text{Fe}(\text{OH})_3$ precipitate was collected by decanting and centrifuging, was dissolved in HCl, digested with HNO_3 , and then ^{210}Po and ^{209}Po were spontaneously plated onto silver plates (Flynn, 1968). The particulate samples collected on the Nuclepore filters were dried in a desiccator and weighed to estimate the concentration of total suspended matter. The filter was then decomposed and digested by a mixture of
25 $\text{HCl}/\text{HF}/\text{HNO}_3/\text{HClO}_4$. The same procedures as for dissolved samples were carried out to plate ^{210}Po and ^{209}Po onto silver plates. The filtered seawater and filter from the 10 L

[Title Page](#)

[Abstract](#)

[Introduction](#)

[Conclusions](#)

[References](#)

[Tables](#)

[Figures](#)

[◀](#)

[▶](#)

[◀](#)

[▶](#)

[Back](#)

[Close](#)

[Full Screen / Esc](#)

[Printer-friendly Version](#)

[Interactive Discussion](#)

subsamples of ^{210}Pb were stored for at least 1 year to let ^{210}Po grow in from ^{210}Pb and the same procedures for dissolved and particulate ^{210}Po were followed.

2.2 Sinking particles

The sinking particles were collected by floating traps in the upper water column, and sinking particles at depths of 700, 1000, 3000, and 3500 m were collected by moored traps (Technicap PPS 5/2; 1 m² collecting area). Selected samples were analyzed for ^{210}Po content by the same procedures as the particulate samples described in the previous section. Separate sets of filters loaded with sinking particles were stored for at least one year to let ^{210}Po grow in from ^{210}Pb and the same procedures for particulate ^{210}Po were followed.

The silver discs were counted by alpha spectrometry (EG&G Ortec 576). After appropriate ingrowth corrections, the ^{210}Pb and ^{210}Po activities in seawater and trap samples at sampling time were calculated

3 Results

Data for total suspended matter (TSM) concentration, dissolved and particulate ^{210}Pb (denoted by $^{210}\text{Pb}_d$ and $^{210}\text{Pb}_p$, respectively), and dissolved and particulate ^{210}Po (denoted by $^{210}\text{Po}_d$ and $^{210}\text{Po}_p$, respectively) are given in Appendix A. Vertical profiles of TSM concentration measured from the four cruises are shown in Fig. 2a, d, g, and k. The TSM falls in a small range of 0.1–0.5 mg L⁻¹ throughout the water column. Vertical distributions of $^{210}\text{Pb}_d$ and $^{210}\text{Pb}_p$ measured from the four cruises are shown in Fig. 2b, e, h, and l. The total ^{210}Pb ($^{210}\text{Pb}_t$) calculated by the summation of $^{210}\text{Pb}_d$ and $^{210}\text{Pb}_p$ is also shown in the figures. Only a small proportion of ^{210}Pb , with an average fraction of ~5 % in the upper 200 m and ~10 % in the deep layer, is associated with particulates.

BGD

11, 11533–11567, 2014

Seasonal distributions and fluxes of ^{210}Pb and ^{210}Po in the Northern South China Sea

C.-L. Wei et al.

Title Page	
Abstract	Introduction
Conclusions	References
Tables	Figures
◀	▶
◀	▶
Back	Close
Full Screen / Esc	
Printer-friendly Version	
Interactive Discussion	

It is noted that, except for the ORI-845 profile, $^{210}\text{Pb}_p$ generally increases with depth, similar to findings in the open ocean (Craig et al., 1973; Somayajulu and Craig, 1976)

Vertical distributions of $^{210}\text{Po}_d$ and $^{210}\text{Po}_p$ measured during the four cruises are shown in Fig. 2c, f, i, and m. The total ^{210}Po ($^{210}\text{Po}_t$) calculated by summing $^{210}\text{Po}_d$ and $^{210}\text{Po}_p$ is also shown in the figures. The $^{210}\text{Po}_d$ is lowest in the mixed layer, increases to a subsurface maximum at 250 m, and then decreases to a relatively constant value of 4 dpm (100 L) $^{-1}$ below the depth of 1000 m. A drastic decrease of $^{210}\text{Po}_d$ in the depth range of 250–1000 m indicates intense scavenging by particles in the twilight zone. Sinking fluxes of total mass (F_{mass}), ^{210}Pb ($F_{\text{Pb-210}}$), and ^{210}Po ($F_{\text{Po-210}}$) measured by the sediment trap are given in Table 1. Our F_{mass} and $F_{\text{Pb-210}}$ are in the range of the temporal data from the site 200 km northeast of the SEATS station (Chung et al., 2004). The $F_{\text{Po-210}}$ showed a large range from $7 \text{ dpm m}^{-2} \text{ d}^{-1}$ at 1000 m to $52.2 \text{ dpm m}^{-2} \text{ d}^{-1}$ at 3000 m.

4 Discussion

15 4.1 Literature data comparison

There are two published ^{210}Po and ^{210}Pb profiles near the SEATS station (Fig. 1). Vertical profiles of $^{210}\text{Po}_t$ and $^{210}\text{Pb}_t$ were reported by Obata et al. (2004) and two sets of dissolved and particulate profiles of ^{210}Pb and ^{210}Po measured in different years were reported by Chung and Wu (2005) in the South China Sea. To compare the consistency of the data, vertical profiles of $^{210}\text{Po}_t$ and $^{210}\text{Pb}_t$ redrawn from the two studies and the average values of the four cruises from this study are shown in Fig. 3. It is noted that the sampling stations of these studies were within 300 km of each other in the semi-enclosed basin of the South China Sea (Fig. 1); an unreasonably large discrepancy exists between the data reported by Chung and Wu (2005) and those of the other two studies. While showing a similar vertical structure, our ^{210}Po data seems

Title Page

Abstract

Introduction

Conclusions

References

Tables

Figures

◀

▶

◀

▶

Back

Close

Full Screen / Esc

Printer-friendly Version

Interactive Discussion

Seasonal distributions and fluxes of ^{210}Pb and ^{210}Po in the Northern South China Sea

C.-L. Wei et al.

systematically lower than Chung and Wu's by 5–10 dpm (100 L) $^{-1}$. The ^{210}Po profile of Obata et al. (2004) is also systematically lower than that of Chung and Wu (2005). The discrepancy is clearly demonstrated by the correlation of $^{210}\text{Po}_t$ and $^{210}\text{Pb}_t$ shown in Fig. 4. It is evident that both $^{210}\text{Pb}_t$ and $^{210}\text{Po}_t$ reported by Chung and Wu (2005) are higher than those of the other two datasets. Not only were systematically higher $^{210}\text{Po}_t$ and $^{210}\text{Pb}_t$ but also a deficiency of ^{210}Po relative to ^{210}Pb , shown as the shaded area in Fig. 3, was found in Chung and Wu (2005). In fact, like many profiles reported in the literature (e.g., Bacon et al., 1976; Sarin et al., 1994), both Obata et al. (2004) and our data showed an excess of ^{210}Po in the layer underlying the euphotic layer. In addition to the vertical profiles, it is also noted that the ^{210}Po data of Nozaki et al. (1998) ($^{210}\text{Po} = 4.2 \text{ dpm (100 L)}^{-1}$, $^{210}\text{Pb} = 6.3 \text{ dpm (100 L)}^{-1}$) measured at the station closest to SEATS in February 1990 and Yang et al.'s (2006) surface ^{210}Po data are close to this study. Moreover, ^{210}Po in the upper 300 m of the western Equatorial Pacific is 6–12 dpm (100 L) $^{-1}$ (Peck and Smith, 2000), which is significantly lower than Chung and Wu's data.

Another line of evidence indicating systematic errors of the ^{210}Pb and ^{210}Po data reported in Chung and Wu (2005) comes from comparison with data from nearby stations in Luzon Strait, which is reported by Chen and Chung (1997) (Fig. 1). We have redrawn $^{210}\text{Pb}_t$ and $^{210}\text{Po}_t$ from stations W3 and W5 of the former study and stations 3 and 7 of the latter study in Fig. 5. A systematic discrepancy was apparently found between the two data sets. Based on comparison of data from the same depth, $^{210}\text{Pb}_t$ and $^{210}\text{Po}_t$ from Chung and Wu (2005) are higher by 10–15 dpm (100 L) $^{-1}$ and 5–10 dpm (100 L) $^{-1}$, respectively, than that of Chen and Chung (1997). Consequently, the systematic error results in an unrealistically large ^{210}Po deficiency in the deep basin of the South China Sea, which leads to the questionable conclusion of Chung and Wu (2005): "Most of the missing ^{210}Po in the upper layer has probably been consumed by bacteria or cyanobacteria and transferred to higher trophic levels of organisms in the food web". The state of $^{210}\text{Pb}/^{226}\text{Ra}$ and $^{210}\text{Po}/^{210}\text{Pb}$ disequilibria in the South China Sea needs to be re-investigated.

[Title Page](#)

[Abstract](#)

[Introduction](#)

[Conclusions](#)

[References](#)

[Tables](#)

[Figures](#)

[◀](#)

[▶](#)

[◀](#)

[▶](#)

[Back](#)

[Close](#)

[Full Screen / Esc](#)

[Printer-friendly Version](#)

[Interactive Discussion](#)

4.2 $^{210}\text{Pb}/^{226}\text{Ra}$ and $^{210}\text{Po}/^{210}\text{Pb}$ disequilibria

To evaluate the degree of deviation of the secular equilibrium, the $\text{SiO}_2-^{226}\text{Ra}$ correlation, $^{226}\text{Ra}(\text{dpm} (100 \text{ L})^{-1}) = 5.15 + 0.14\text{SiO}_2 (\mu\text{mol L}^{-1})$, which is based on the data determined at station PA-11 by Nozaki and Yamamoto (2001) (Fig. 1), is used to calculate ^{226}Ra activity. Vertical profiles of the $^{210}\text{Pb}_t/^{226}\text{Ra}$ ratio obtained from the four cruises to the SEATS station are shown in Fig. 6a. Due to atmospheric input, an excess of ^{210}Pb relative to ^{226}Ra in the upper 250 m is generally found. In contrast to the upper water column, ^{210}Pb shows a large deficiency relative to ^{226}Ra in the deep water, indicating fast removal of ^{210}Pb in the deep basin of the South China Sea. Similar to the findings in the open ocean (Bacon et al., 1976), the average $^{210}\text{Pb}_t/^{226}\text{Ra}$ ratio decreases dramatically in the thermocline then maintains a constant value of 0.5 below 1000 m. Compared to the values summarized in the compilation of Nozaki et al. (1997), the $^{210}\text{Pb}_t/^{226}\text{Ra}$ ratio is higher than that found in the Bay of Bengal (Cochran et al., 1983; Sarin et al., 1994), the Bismarck Sea (Nozaki et al., 1997) and the Sea of Japan (Nozaki et al., 1973) but lower than in the deep water of the North Pacific (Craig et al., 1973; Nozaki et al., 1980) and the North Atlantic (Bacon et al., 1976). Minor differences of the ratio seem to exist among cruises, however, the variation is too small to reveals apparent temporal variation. The $^{210}\text{Pb}_t/^{226}\text{Ra}$ ratio showed a decreasing trend toward sediments in the bottom layer, indicating intensified scavenging at the water–sediment interface (Spencer et al., 1980). This boundary-scavenging phenomenon was also reported in the North Pacific (Nozaki et al., 1980), the Indian Ocean (Cochran et al., 1983), and the continental slope of the South Atlantic Bight (Bacon et al., 1988).

Vertical profiles of the $^{210}\text{Po}_t/^{210}\text{Pb}_t$ ratio of the four cruises to the SEATS station are shown in Fig. 6b. The general pattern of ^{210}Po distribution shows a deficiency in the surface layer and an excess in the thermocline, similar to the phenomenon observed in the open ocean (Bacon et al., 1976). It can be seen that the deficiency of ^{210}Po in the thermocline varies greatly among cruises, indicating temporal variation of ^{210}Po regeneration caused by particle decomposition in the twilight zone of the water column. On the

Title Page

Abstract

Introduction

Conclusions

References

Tables

Figures

◀

▶

◀

▶

Back

Close

Full Screen / Esc

Printer-friendly Version

Interactive Discussion

contrary, in the water column deeper than 1000 m, a relatively constant $^{210}\text{Po}_t/^{210}\text{Pb}_t$ ratio of 0.75 was found, which is similar to the ratio found in the Santa Monica Basin (0.72, Wong et al., 1992), the Okinawa Trough (0.71, Nozaki et al., 1990), the eastern South Pacific (0.80, Thomson and Turekian, 1976), and the Sargasso Sea (0.70, Kim and Church, 2001). Recent results of an inter-calibration project also showed a significant deficiency of ^{210}Po relative to ^{210}Pb in the deep water, with a $^{210}\text{Po}/^{210}\text{Pb}$ ratio of 0.74 ± 0.06 at 2000 m at BATS in the North Atlantic and 0.80 ± 0.11 at 3000 m at the baseline station in the North Pacific, respectively (Church et al., 2012). It should be noted that, contrary to the ^{210}Po deficiencies in these environments, the $^{210}\text{Po}_t/^{210}\text{Pb}_t$ ratio is commonly close to unity in the deep layer (> 1000 m) of the ocean (1988; Bacon et al., 1976; Cochran et al., 1983; Nozaki et al., 1997).

The inventories of dissolved and particulate ^{210}Pb and ^{210}Po in the water column above the four depths from the four cruises are presented in Table 2. The average inventories of total ^{210}Pb and total ^{210}Po in the upper 1000 m are $85.5 \times 10^3 \text{ dpm m}^{-2}$ and $64.7 \times 10^3 \text{ dpm m}^{-2}$, respectively, which result in an integrated ^{210}Po deficit of $20.7 \times 10^3 \text{ dpm m}^{-2}$. Significantly higher ^{210}Po deficits were found in the Philippine Sea, $86 \times 10^3 \text{ dpm m}^{-2}$, and in the Okinawa Trough, $118 \times 10^3 \text{ dpm m}^{-2}$, which was attributed to the focusing effect of ^{210}Pb accumulation by Kuroshio transport (Nozaki et al., 1990). In the oligotrophic Sargasso Sea, Kim (2001) also found a much higher ^{210}Po deficit of $56 \times 10^3 \text{ dpm m}^{-2}$ due to an unexpectedly high ^{210}Pb inventory of $135 \times 10^3 \text{ dpm m}^{-2}$ in the upper 1000 m, which was attributed to the process of ^{210}Po being transported by macrozooplankton instead of removed by particle settling. On the contrary, the ^{210}Po deficit in the South China Sea is higher than those found in the eastern South Pacific (5×10^3 – $15 \times 10^3 \text{ dpm m}^{-2}$, (Thomson and Turekian, 1976) and comparable with those found in the western Equatorial Pacific (26×10^3 – $43 \times 10^3 \text{ dpm m}^{-2}$, Nozaki et al., 1997). A higher deficiency of ^{210}Po compared to the open ocean implies faster removal by particle settling in the South China Sea.

Both the South China Sea and Sea of Japan are semi-enclosed marginal seas with limited exchange with the open ocean; hence, it is interesting to compare the ^{210}Pb –

Seasonal distributions and fluxes of ^{210}Pb and ^{210}Po in the Northern South China Sea

C.-L. Wei et al.

[Title Page](#)

[Abstract](#)

[Introduction](#)

[Conclusions](#)

[References](#)

[Tables](#)

[Figures](#)

[◀](#)

[▶](#)

[◀](#)

[▶](#)

[Back](#)

[Close](#)

[Full Screen / Esc](#)

[Printer-friendly Version](#)

[Interactive Discussion](#)

²¹⁰Po systematics in the two basins. However, only ²¹⁰Po data is available in the deep water of the Sea of Japan, in which ²¹⁰Po inventories ranged from 43.5×10^3 to 65.8×10^3 dpm m⁻² and from 78.2×10^3 to 100.6×10^3 dpm m⁻² in the upper 1000 m and 2000 m, respectively (Hong et al., 2008). Our results of ²¹⁰Po inventories in the upper 5 1000 m of the South China Sea are comparable with those from the Sea of Japan. However, compared with the 138.9×10^3 dpm m⁻² in the water column above 2000 m of the South China Sea, the ²¹⁰Po inventories are 40–60 % lower in the Sea of Japan, which, as described in Hong et al. (2008), may be caused by enhanced removal by 10 terrestrial inputs of particles. Unfortunately, no ²¹⁰Pb data is available for revealing the degree of ²¹⁰Pb–²¹⁰Po disequilibrium in the deep water of the Sea of Japan.

4.3 Partitioning of ²¹⁰Pb and ²¹⁰Po in dissolved and particulate phases

Although both are particle-reactive, subtle differences are found for ²¹⁰Po and ²¹⁰Pb in the interaction with particles in the ocean. It is known that ²¹⁰Po shows a higher affinity to organic particles whereas ²¹⁰Pb tends to associate with inorganic particles 15 (Bacon et al., 1976; Shannon et al., 1970). A shorter residence time is found for ²¹⁰Po compared to ²¹⁰Pb in the surface ocean (Nozaki et al., 1998), which reflects the relative intensity of interaction between the two radionuclides and particulate matter. The vertical profiles (Fig. 2) showed that, except in the subsurface water underlying the euphotic layer, ²¹⁰Po is lower than ²¹⁰Pb in the dissolved phase whereas the opposite 20 was found in the particulate phase, leading to a higher percentage of ²¹⁰Po than ²¹⁰Pb being associated with particles.

The partition coefficients of ²¹⁰Pb and ²¹⁰Po, $K_d(\text{Pb})$ and $K_d(\text{Po})$, respectively, have been used as an indicator of the affinities of radionuclides for particulate matter (Bacon

[Title Page](#)[Abstract](#)[Introduction](#)[Conclusions](#)[References](#)[Tables](#)[Figures](#)[◀](#)[▶](#)[◀](#)[▶](#)[Back](#)[Close](#)[Full Screen / Esc](#)[Printer-friendly Version](#)[Interactive Discussion](#)

et al., 1976; Wei and Murray, 1994). The two coefficients can be calculated by

$$K_d(\text{Pb}) = \frac{^{210}\text{Pb}_p}{^{210}\text{Pb}_d \times \text{TSM}} \times 10^6 \quad (1)$$

$$K_d(\text{Po}) = \frac{^{210}\text{Po}_p}{^{210}\text{Po}_d \times \text{TSM}} \times 10^6 \quad (2)$$

- 5 The vertical profiles of $K_d(\text{Pb})$ and $K_d(\text{Po})$ are shown in Fig. 7. The K_d values fall in the range of $10^{5.0}\text{--}10^{6.8} \text{ mL g}^{-1}$ and $10^{4.7}\text{--}10^{7.2} \text{ mL g}^{-1}$ for ^{210}Pb and ^{210}Po , respectively. Based on the average value of K_d , ^{210}Po shows a higher affinity to particles, which is consistent with the results in the western North Atlantic (Bacon et al., 1988), the Equatorial Pacific (Murray et al., 2005), and the Arabian Sea (Sarin et al., 1994). A broad
10 subsurface minimum of $K_d(\text{Po})$ underlying the euphotic layer was found, which is similar to the findings in the Sea of Japan (2008). The minimum can be ascribed to the process of particle decomposition and remineralization (Bacon et al., 1976; Hong et al., 2008).

15 The fractionation factor, $F_{\text{Po/Pb}}$, was used by Bacon et al. (1988) to compare the relative affinity of ^{210}Po and ^{210}Pb to the particles. $F_{\text{Po/Pb}}$ is calculated by

$$F_{\text{Po/Pb}} = \frac{K_d(\text{Po})}{K_d(\text{Pb})} = \frac{^{210}\text{Po}_p \times ^{210}\text{Pb}_d}{^{210}\text{Po}_d \times ^{210}\text{Pb}_p} \quad (3)$$

The vertical distribution of $F_{\text{Po/Pb}}$ is shown in Fig. 7b. Except in the subsurface layer underlying the euphotic zone in October, $F_{\text{Po/Pb}}$ is greater than unity in the whole water column.

20 There are limited data on the partitioning of ^{210}Pb and ^{210}Po in the dissolved and particulate phases for calculation of $K_d(\text{Pb})$ and $K_d(\text{Po})$ in the deep basin of the open ocean. The compilation of literature data from the deep ocean on the correlations of $K_d(\text{Pb})$ and $K_d(\text{Po})$ with TSM are shown in Fig. 8a and b, respectively. Unlike the findings in the Yellow Sea (Hong et al., 1999) and coastal waters with high particle

Title Page

Abstract

Introduction

Conclusions

References

Tables

Figures

◀

▶

◀

▶

Back

Close

Full Screen / Esc

Printer-friendly Version

Interactive Discussion

loads (Wei et al., 2012), an inverse relationship between K_d and the concentration of TSM are evident in the open ocean. The negative correlation between the K_d s and the TSM indicates the partitioning between dissolved and particulate phases in the deep ocean is controlled by particle-particle interactions, which was proposed by Honeyman et al. (1988) and Honeyman and Santschi (1989) based on ^{234}Th data in the ocean. In the context of the Browning pumping model (Honeyman and Santschi, 1989), scavenging of particle-reactive elements in the deep ocean that are characterized by extremely low particle concentrations is controlled by slow particle-particle interactions and the slope of the logTSM-logKd correlation reflects the fraction of elements associated with colloids in filterable pool.

Nozaki et al. (1998) reported ^{210}Pb and ^{210}Po activities in the surface water at three stations in the South China Sea. Compared with other regions, as a result of low biological activity and the terrestrial input of detrital material, Nozaki et al. (1998) found ^{210}Po is removed at a faster rate than ^{210}Pb in the South China Sea. Due to this fractionation, the predicted $^{210}\text{Po}/^{210}\text{Pb}$ ratio in sinking particles is only 0.58, lower than that in other regions. Corroborating with the prediction of Nozaki et al. (1998), Chung and Wu (2005) found that the $^{210}\text{Po}/^{210}\text{Pb}$ in suspended particles collected from the euphotic layer at SEATS ranges from 0.66 to 0.77.

4.4 Sinking fluxes of ^{210}Pb and ^{210}Po

There are two major sources of ^{210}Pb in the ocean: radioactive decay of ^{226}Ra in seawater and atmospheric ^{210}Pb input via dry and wet deposition into the surface layer (Bacon et al., 1976). Hence, assuming a steady state, the removal flux of ^{210}Pb via particle settling can be estimated by

$$F_{\text{Pb-210}} = I_{\text{Pb-210}} + \lambda_1 \sum (\text{Ra} - \text{Pb}_t) \quad (4)$$

where $F_{\text{Pb-210}}$ is the removal flux, $I_{\text{Pb-210}}$ is the atmospheric ^{210}Pb deposition flux, λ_1 is the radioactive decay constant of ^{210}Pb ($= 8.48 \times 10^{-5} \text{ d}^{-1}$), and the summation

symbol represents the inventory of the radionuclides. It should be pointed out that the steady-state assumption is justified by the small temporal variation of the ^{210}Pb inventory in the whole water column of the SEATS site (Table 2). The atmospheric ^{210}Pb flux at the sampling site is not known; however, taking the average value of 0.4 dpm $\text{cm}^{-2} \text{a}^{-1}$ by Feichter et al. (1991) and 0.76 dpm $\text{cm}^{-2} \text{yr}^{-1}$ by Xu et al. (2010), an $I_{\text{Pb-210}}$ of 0.6 dpm $\text{cm}^{-2} \text{yr}^{-1}$ ($16.4 \text{ dpm m}^{-2} \text{d}^{-1}$) was assumed in the southern South China Sea (Wei et al., 2011). The $F_{\text{Pb-210}}$ estimated from the ^{210}Pb deficiencies in the water column falls in relatively small ranges, which are 30.5–32.1, 40.3–44.6, and 44.5–51.3 dpm $\text{m}^{-2} \text{d}^{-1}$, above 2000 m, 3000 m, and 3500 m, respectively. The ^{210}Pb flux measured from the sediment trap samples, which showed an average value of 34.3 dpm $\text{m}^{-2} \text{d}^{-1}$ at 3000 m and 46.3 dpm $\text{m}^{-2} \text{d}^{-1}$ at 3500 m (Table 1), are generally in agreement with the estimated values. Similar ^{210}Pb flux predicted from the deficiency of ^{210}Pb in the water column to the $F_{\text{Pb-210}}$ measured by the sediment trap indicates that removal by particle settling instead of bottom scavenging at the water–sediment interface is the dominant process for ^{210}Pb removal in the South China Sea.

In most studies (e.g., Bacon et al., 1976; Hong et al., 2008; Nozaki et al., 1990; Obata et al., 2004), steady-state was generally assumed to estimate the scavenging flux ($J_{\text{Po-210}}$) and removal flux ($F_{\text{Po-210}}$) of ^{210}Po in the deep ocean by

$$J_{\text{Po-210}} = \lambda_2 \sum (\text{Pb}_d - \text{Po}_d) \quad (5)$$

$$F_{\text{Po-210}} = \lambda_2 \sum (\text{Pb}_t - \text{Po}_t) \quad (6)$$

where λ_2 is decay constant of ^{210}Po ($= 0.005 \text{ d}^{-1}$).

However, time-series profiles of dissolved and particulate ^{210}Pb and ^{210}Po have enabled us to estimate the scavenging and removal fluxes of ^{210}Po without assuming steady state. Even in a deep basin like the Sea of Japan, Hong et al. (2008) found that temporal variation of ^{210}Po profiles may occur. They found that the inventory of total ^{210}Po may decrease by 15 % during a period of six months at the same site in the deep basin of the Sea of Japan (Hong et al., 2008). Unfortunately, except for the data

Seasonal distributions and fluxes of ^{210}Pb and ^{210}Po in the Northern South China Sea

C.-L. Wei et al.

[Title Page](#)

[Abstract](#)

[Introduction](#)

[Conclusions](#)

[References](#)

[Tables](#)

[Figures](#)

[◀](#)

[▶](#)

[◀](#)

[▶](#)

[Back](#)

[Close](#)

[Full Screen / Esc](#)

[Printer-friendly Version](#)

[Interactive Discussion](#)

reported by Kim and Church (2001) in the upper 500 m of the Sargasso Sea, no systematic time-series of ^{210}Pb and ^{210}Po data had been available to evaluate the effect of temporal variation on particle removal in the deep basins of the ocean. Following the formulation of Kim and Church (2001), neglecting atmospheric input and taking into account temporal variation, the equations for the scavenging flux and removal flux of ^{210}Po are given by

$$J_{\text{Po-210}} = \lambda_2 \left[\frac{\sum \text{Pb}_d (1 - e^{-\lambda_2 \Delta t}) + \sum \text{Po}_d^{t_1} e^{-\lambda_2 \Delta t} - \sum \text{Po}_d^{t_2}}{1 - e^{-\lambda_2 \Delta t}} \right] \quad (7)$$

$$F_{\text{Po-210}} = \lambda_2 \left[\frac{\sum \text{Pb}_t (1 - e^{-\lambda_2 \Delta t}) + \sum \text{Po}_t^{t_1} e^{-\lambda_2 \Delta t} - \sum \text{Po}_t^{t_2}}{1 - e^{-\lambda_2 \Delta t}} \right] \quad (8)$$

where the summation symbol represents the inventory of radionuclides and Δt is the interval between consecutive sampling times designated by superscripts t_1 and t_2 . The results of scavenging and removal fluxes calculated by steady-state (SS) and non-steady-state (NSS) at four depths were shown in Fig. 8, in which the uncertainty was estimated based on the propagation of error. There were four sampling periods available for the estimation of the sinking flux of ^{210}Po at 1000 m, whereas only three sets of profiles were available for the modeling task at depths deeper than 1000 m. Several inferences can be made regarding the scavenging and removal fluxes of ^{210}Po in the South China Sea:

1. except for the $J_{\text{Po-210}}$ flux at 1000 m in June 2007, both $J_{\text{Po-210}}$ and $F_{\text{Po-210}}$ calculated from the steady-state and the non-steady-state models showed little difference within the uncertainty, indicating a minor effect of temporal variation on the scavenging and removal of ^{210}Po in the deep layer,

Title Page	
Abstract	Introduction
Conclusions	References
Tables	Figures
◀	▶
◀	▶
Back	Close
Full Screen / Esc	
Printer-friendly Version	
Interactive Discussion	

2. seasonal variation of $J_{\text{Po-210}}$ and $F_{\text{Po-210}}$ fluxes at 1000 m was found, implying the scavenging and removal of ^{210}Po may be controlled by production and decomposition of biological particles in the euphotic layer, and
- 5 3. a general increasing trend with depth was found for both $J_{\text{Po-210}}$ and $F_{\text{Po-210}}$. The largest increase rate was found between 1000 m and 2000 m, indicating ^{210}Po is continuously scavenged while particles sink through the water column.

One independent method with which to check the validity of the model estimates is to compare the flux estimates with directly measured sinking fluxes from sediment traps. Although limited ^{210}Po measurements were made on the sinking particles collected by the sediment trap, the data listed in Table 1 provide an independent check of the sinking fluxes of ^{210}Po . The $F_{\text{Po-210}}$ calculated by Eq. (8) is 412–470 dpm $\text{m}^{-2} \text{d}^{-1}$ at 3000 m and 481–567 dpm $\text{m}^{-2} \text{d}^{-1}$ at 3500 m, which is much higher than the measured flux by more than one order of magnitude (Table 1). In the Santa Monica Basin, Wong et al. (1992) also found the measured ^{210}Po flux by sediment traps was significantly lower than the predicted ^{210}Po flux from the $^{210}\text{Po}/^{210}\text{Pb}$ disequilibrium in the water column. The large discrepancy suggests three possible causes: (1) under-trapping of sediment traps, (2) ^{210}Po removal by processes other than particle sinking, and (3) episodic particle removals not caught by sediment traps. Since the current velocity in the deep layer (3000 m) of the South China Sea is low ($0.5\text{--}2 \text{ cm s}^{-1}$, Wang et al., 2011) and, as discussed previously, ^{210}Pb fluxes in agreement between trap-measured and modeled fluxes were found, it is very unlikely that the discrepancy of predicted and measured fluxes is caused by under-trapping of the sediment traps. To explain a larger deficiency of ^{210}Po with respect to ^{210}Pb in the water column of oligotrophic regimes compared to that in more productive regimes, Kim (2001) proposed a very different view on the mechanism of polonium removal from the ocean, i.e., instead of the conventional view that polonium is removed by settling particles, the large ^{210}Po deficiency found in oligotrophic ocean was attributed to efficient uptake by cyanobacteria and transfer to higher trophic levels. Based on the questionable data, Chung and Wu (2005) also

Seasonal distributions and fluxes of ^{210}Pb and ^{210}Po in the Northern South China Sea

C.-L. Wei et al.

[Title Page](#)[Abstract](#)[Introduction](#)[Conclusions](#)[References](#)[Tables](#)[Figures](#)[◀](#)[▶](#)[◀](#)[▶](#)[Back](#)[Close](#)[Full Screen / Esc](#)[Printer-friendly Version](#)[Interactive Discussion](#)

ascribed the ^{210}Po removal to trophic transfer in the South China Sea. However, Hong et al. (2013) recently reported results of ^{210}Po flux data measured by sediment traps in the deep layer of the oligotrophic basin at the BATS station, which was similar to the ^{210}Po fluxes calculated from the water-column deficiency. In the context of Kim (2001), to balance the amount of ^{210}Po removed by swimmers, a large quantity of excess ^{210}Po would exist somewhere in the South China Sea to balance the “missing flux” that was transported away from the SEATS site by nekton via cyanobacterial uptake of ^{210}Po . This hypothesis can only be tested with more profiles to reveal the spatial variability of the distributions of ^{210}Po and ^{210}Pb in the South China Sea.

We propose that sporadic wash-out by calcareous ballasts poses a plausible cause of the large discrepancy between the modeled ^{210}Po flux and the measured flux at the site. Chen et al. (2007) investigated the spatial and temporal variation of coccolithophore biomass and the vertical fluxes of coccolithophores in the northern South China Sea. Induced by nutrient inputs associated with the northeast monsoon, coccolithophore abundance significantly increased during the winter, which resulted in a 6-fold increase in the sinking flux of calcareous coccoliths in comparison with the summer in the deep layer of the SEATS site (Chen et al., 2007). The $F_{\text{Po-210}}$ listed in Table 1 only represented the average flux during a 15 day period, the duration set by the rotary sampler of the sediment trap, during January and July of 2007. It is possible a much higher flux of ^{210}Po -laden particles was missed. Sherrell et al. (1998) proposed episodic particle sweeping events to explain the temporal variation of suspended particle concentrations in the water column off California. The TSM profiles shown in Fig. 2 display the temporal variation. The inventories of TSM can vary by 30 %, from 23 to 31 g m^{-2} , in the upper 1000 m and by 20 %, from 817 to 972 g m^{-2} , in the whole 3500 m water column, depicting sporadic events that strip particles from the water column. Nonetheless, no conclusive proof can be made yet until more flux data are available to demonstrate the temporal variation of ^{210}Po flux in the deep layer. This result warrants continuous measurements of the sinking flux using sediment traps deployed in the deep layer of the basin to investigate the ^{210}Po removal by particle settling in the South China Sea.

4.5 Residence times of ^{210}Pb and ^{210}Po

The residence time of ^{210}Pb with respect to the particle removal rate in the deep ocean shows a large range, from 2–3 yr in anoxic basins to 300 yr in the central gyre of the Pacific (Nozaki et al., 1997). The residence time of ^{210}Pb , τ_{Pb} , with respect to particle removal was calculated by dividing the inventories of $^{210}\text{Pb}_t$ by the $F_{\text{Pb-210}}$ from Eq (4). The τ_{Pb} ranges from 12 to 17 yr in the deep layer of the South China Sea, which is consistent with the value estimated by Obata et al. (2004). The τ_{Pb} in the South China Sea is also comparable with the values reported in other marginal seas of the western North Pacific like the East China Sea and the Sea of Japan, in which an average residence time of 15 yr was estimated (Nozaki et al., 1990, 1973). In the deep layer of the Bismarck Sea and the Bay of Bengal, a very short τ_{Pb} of 8 yr was reported (Cochran et al., 1983; Nozaki et al., 1997). A shorter residence time of ^{210}Pb in marginal seas than in the open ocean, which is about 50–300 yr (Bacon et al., 1976; Chung and Craig, 1983; Craig et al., 1973; Nozaki and Tsunogai, 1976; Nozaki et al., 1997), demonstrates the boundary scavenging phenomenon incurred by enhanced particle removal in the regions near land masses. It is noted that the τ_{Pb} in the deep basin is shorter than the mixing time required for the water exchange between the western Pacific and the South China Sea. Residence times of 100 yr based on ^{14}C tracer (Broecker et al., 1986) and 30–71 yr based on deep water transport (Chang et al., 2010) were estimated for the seawater in the South China Sea. Shorter τ_{Pb} than the residence time of water implies a lower ^{210}Pb concentration in the South China Sea than in the western Philippine Sea. Indeed, compared with data from the eastern Luzon Strait, from which the deep water of the South China Sea originates (Gong et al., 1992), our unpublished data showed that the $^{210}\text{Pb}_t$ is about 5–10 dpm (100 L) $^{-1}$ lower in the deep water of the South China Sea.

Similarly, the residence time of ^{210}Po , τ_{Po} , with respect to particle removal was calculated by dividing the inventories of $^{210}\text{Po}_t$ by the $F_{\text{Po-210}}$ from Eq. (6) and Eq. (8), based on the SS and NSS models, respectively. Since the temporal variation of ^{210}Po

[Title Page](#)[Abstract](#)[Introduction](#)[Conclusions](#)[References](#)[Tables](#)[Figures](#)[◀](#)[▶](#)[◀](#)[▶](#)[Back](#)[Close](#)[Full Screen / Esc](#)[Printer-friendly Version](#)[Interactive Discussion](#)

inventory in the water column is not large enough to significantly affect the $F_{\text{Po-210}}$ calculation, the τ_{Po} calculated by either the SS or NSS models showed no significant difference. The residence time of ^{210}Po ranged from 0.9 to 2.2 yr for the upper 1000 m and from 1.2 to 1.7 yr for the upper 3000 m of the water column. Except in regions of high productivity, the disequilibrium of ^{210}Po and ^{210}Pb is not evident in the deep layer of the open ocean, hence, a longer residence time of ^{210}Po with respect to particle removal, 2–4 yr, was estimated (Bacon et al., 1976; Thomson and Turekian, 1976). Even in marginal seas, a relatively long residence time of ^{210}Po was found in deep water. For example, Hong et al. (2008) estimated the τ_{Po} of 2.3–5.5 yr in the Japan Sea and Wong et al. (1992) reported the τ_{Po} of 3.2 yr in the Santa Monica Basin. Compared with literature results found in the open ocean and other marginal seas, the τ_{Po} in deep water is smaller, indicating enhanced ^{210}Po removal from the water column of the South China Sea. We speculate the enhancement is related to the episodic settling of coccolithophore ballast, which may serve as an efficient carrier of organic particles and associated ^{210}Po .

5 Conclusions

This study reported the vertical profiles of dissolved and particulate ^{210}Pb and ^{210}Po at the time-series station, SEATS, in the South China Sea. The time-series ^{210}Pb and ^{210}Po data allow us to evaluate the importance of temporal variations of particle removal in the deep basin of the South China Sea.

Limited data of ^{210}Pb and ^{210}Po concentrations in the sinking particles collected by the sediment traps showed that the measured ^{210}Pb flux is consistent with the removal rate predicted from the ^{210}Pb – ^{226}Ra deficiency whereas the measured ^{210}Po flux is significantly lower than the expected removal from the ^{210}Po – ^{210}Pb deficiency in the water column. Future studies aimed at sediment trap deployments in the deep basin to reveal temporal variability of the ^{210}Po sinking flux are warranted. A short residence time, 12–17 yr, relative to the particle removal rate was estimated for ^{210}Pb in the deep

Title Page	Abstract	Introduction
Conclusions	References	
Tables	Figures	
◀	▶	
◀	▶	
Back	Close	
Full Screen / Esc		
Printer-friendly Version		
Interactive Discussion		

basin of the South China Sea. The significantly shorter residence time than that found in the open ocean demonstrates the boundary scavenging effect caused by enhanced scavenging at the water–sediment interface.

BGD

11, 11533–11567, 2014

Acknowledgements. This study was supported by the National Science Council under grants NSC 102-2611-M-002-007-MY3. We would also like to thank the technical group of the SEATS program of NCOR for their excellent work in measuring hydrographic parameters.

References

- Bacon, M. P., Spencer, D. W., and Brewer, P. G.: $^{210}\text{Pb}/^{226}\text{Ra}$ and $^{210}\text{Po}/^{210}\text{Pb}$ disequilibria in seawater and suspended particulate matter, *Earth Planet. Sc. Lett.*, 32, 277–299, 1976.
- Bacon, M. P., Belastock, R. A., Tecotzky, R. A. M., Turekian, K. K., and Spencer, D. W.: Lead-210 and polonium-210 in ocean water profiles of the continental shelf and slope south of New England, *Cont. Shelf Res.*, 8, 841–853, 1988.
- Broecker, W. S., Patzert, W. C., Toggweiler, J. R., and Stuiver, M.: Hydrography, chemistry, and radioisotopes in the southeast Asian basins, *J. Geophys. Res.*, 91, 14345–14354, 1986.
- Chang, Y.-T., Hsu, W.-L., Tai, J.-H., Tang, T.-Y., Chang, M.-H., and Chao, S.-Y.: Cold Deep Water in the South China Sea, *J. Oceanogr.*, 66, 183–190, 2010.
- Chen, J.-N. and Chung, Y.: ^{226}Ra , ^{210}Pb and ^{210}Po distributions at the sea off Southern Taiwan: radioactive disequilibria and temporal variations, *Terr. Atmos. Ocean. Sci.*, 8, 255–270, 1997.
- Chen, Y.-L. L., Chen, H.-Y., and Chung, C.-W.: Seasonal variability of coccolithophore abundance and assemblage in the northern South China Sea, *Deep-Sea Res. Pt. II*, 54, 1617–1633, 2007.
- Cherry, R. D., Fowler, S. W., Beasley, T. M., and Heyraud, M.: Polonium-210: its vertical oceanic transport by zooplankton metabolic activity, *Mar. Chem.*, 3, 105–110, 1975.
- Chung, Y. and Craig, H.: Pb-210 in the Pacific – the GEOSECS measurements of particulate and dissolved concentrations, *Earth Planet. Sc. Lett.*, 65, 406–432, 1983.
- Chung, Y. and Wu, T.: Large ^{210}Po deficiency in the northern South China Sea, *Cont. Shelf Res.*, 25, 1209–1224, 2005.

Seasonal distributions and fluxes of ^{210}Pb and ^{210}Po in the Northern South China Sea

C.-L. Wei et al.

[Title Page](#)

[Abstract](#)

[Introduction](#)

[Conclusions](#)

[References](#)

[Tables](#)

[Figures](#)

◀

▶

◀

▶

[Back](#)

[Close](#)

[Full Screen / Esc](#)

[Printer-friendly Version](#)

[Interactive Discussion](#)

Seasonal
distributions and
fluxes of ^{210}Pb and
 ^{210}Po in the Northern
South China Sea

C.-L. Wei et al.

- Chung, Y., Chang, H. C., and Hung, G. W.: Particulate flux and ^{210}Pb determined on the sediment trap and core samples from the northern South China Sea, *Cont. Shelf Res.*, 24, 673–691, 2004.
- Church, T., Rigaud, S., Baskaran, M., Kumar, A., Friedrich, J., Masque, P., Puigcorbé, V., Kim, G., Radakovitch, O., Hong, G., Choi, H., and Stewart, G.: Intercalibration studies of ^{210}Po and ^{210}Pb in dissolved and particulate seawater samples, *Limnol. Oceanogr.-Meth.*, 10, 776–789, 2012.
- Cochran, J. K. and Masque, P.: Short-lived U/Th series radionuclides in the ocean: tracers for scavenging rates, export fluxes and particle dynamics, *Rev. Mineral. Geochem.*, 52, 461–492, 2003.
- Cochran, J. K., Bacon, M. P., Krishnaswami, S., and Turekian, K. K.: Po-210 and Pb-210 distributions in the central and eastern Indian Ocean, *Earth Planet. Sc. Lett.*, 65, 433–452, 1983.
- Craig, H., Krishnaswami, S., and Somayajulu, B. L. K.: Pb-210–Ra-226 radioactive disequilibrium in deep sea, *Earth Planet. Sc. Lett.*, 17, 295–305, 1973.
- Feichter, J., Brost, R. A., and Heimann, M.: 3-dimensional modeling of the concentration and deposition of Pb-210 aerosols, *J. Geophys. Res.*, 96, 22447–22460, 1991.
- Fisher, N. S., Cochran, J. K., Krishnaswami, S., and Livingston, H. D.: Precicting the oceanic flux of radionuclides on sinking biogenic debris, *Nature*, 335, 622–625, 1988.
- Flynn, W. W.: The determination of low levels of polonium-210 in environmental materials, *Anal. Chim. Acta*, 43, 221–227, 1968.
- Gong, G.-C., Liu, K.-K., Liu, C.-T., and Pai, S.-C.: The chemical hydrography of the South China Sea west of Luzon and a comparison with the West Philippine Sea, *Terr. Atmos. Ocean. Sci.*, 3, 587–602, 1992.
- Honeyman, B. D. and Santschi, P. H.: A Brownian-pumping model for oceanic trace metal scavenging: evidence from Th isotopes, *J. Mar. Res.*, 47, 951–992, 1989.
- Honeyman, B. D., Balistrieri, L. S., and Murray, J. W.: Oceanic trace metal scavenging: the importance of particle concentration, *Deep-Sea Res.*, 35, 227–246, 1988.
- Hong, G.-H., Park, S.-K., Baskaran, M., Kim, S.-H., Chung, C.-S., and Lee, S.-H.: Lead-210 and polonium-210 in the winter well-mixed turbid waters in the mouth of the Yellow Sea, *Cont. Shelf Res.*, 19, 1049–1064, 1999.
- Hong, G.-H., Kim, Y.-I., Baskaran, M., Kim, S.-H., and Chung, C.-S.: Distribution of ^{210}Po and export of organic carbon from the euphotic zone in the southwestern East Sea (Sea of Japan), *J. Oceanogr.*, 64, 277–292, 2008.

[Title Page](#)

[Abstract](#)

[Introduction](#)

[Conclusions](#)

[References](#)

[Tables](#)

[Figures](#)

◀

▶

◀

▶

[Back](#)

[Close](#)

[Full Screen / Esc](#)

[Printer-friendly Version](#)

[Interactive Discussion](#)

Seasonal distributions and fluxes of ^{210}Pb and ^{210}Po in the Northern South China Sea

C.-L. Wei et al.

[Title Page](#)

[Abstract](#)

[Introduction](#)

[Conclusions](#)

[References](#)

[Tables](#)

[Figures](#)

◀

▶

◀

▶

[Back](#)

[Close](#)

[Full Screen / Esc](#)

[Printer-friendly Version](#)

[Interactive Discussion](#)



Seasonal
distributions and
fluxes of ^{210}Pb and
 ^{210}Po in the Northern
South China Sea

C.-L. Wei et al.

- Peck, G. A. and Smith, J. D.: Distribution of dissolved and particulate ^{226}Ra , ^{210}Pb and ^{210}Po in the Bismarck Sea and western equatorial Pacific Ocean, *Marine Freshwater Research*, 51, 647–658, 2000.
- Sarin, M., Rengarajan, R., and Somayajulu, B. L. K.: Natural radionuclides in the Arabian Sea and Bay of Bengal: distribution and evaluation of particle scavenging processes, *P. Indian Acad. Sci.*, 103, 211–235, 1994.
- Shannon, L. V., Cherry, R. D., and Orren, M. J.: Polonium-210 and lead-210 in the marine environment, *Geochim. Cosmochim. Ac.*, 34, 701–711, 1970.
- Sherrell, R. M., Field, M. P., and Gao, Y.: Temporal variability of suspended mass and composition in the Northeast Pacific water column: relationships to sinking flux and lateral advection, *Deep-Sea Res. Pt. II*, 45, 733–761, 1998.
- Somayajulu, B. L. K. and Craig, H.: Particulate and soluble ^{210}Pb activities in the deep sea, *Earth Planet. Sc. Lett.*, 32, 268–276, 1976.
- Spencer, D. W., Bacon, M. P., and Brewer, P. G.: The distribution of ^{210}Pb and ^{210}Po in the North Sea, *Thalassia Jugoslavica*, 16, 125–154, 1980.
- Thomson, J. and Turekian, K. K.: ^{210}Po and ^{210}Pb distributions in ocean water profiles from the eastern South Pacific, *Earth Planet. Sc. Lett.*, 32, 297–303, 1976.
- Tseng, C. M., Wong, G. T. F., Lin, I. I., Wu, C. R., and Liu, K. K.: A unique seasonal pattern in phytoplankton biomass in low-latitude waters in the South China Sea, *Geophys. Res. Lett.*, 32, L08608, doi:10.1029/2004GL022111, 2005.
- Turekian, K. K., Nozaki, Y., and Benniger, L.: Geochemistry of atmospheric radon and radon products, *Annu. Rev. Earth Pl. Sc.*, 5, 227–255, 1977.
- Wang, G., Xie, S.-P., Qu, T. D., and Huang, R. X.: Deep South China Sea circulation, *Geophys. Res. Lett.*, 38, L05601, doi:10.1029/2010GL046626, 2011.
- Wei, C.-L. and Murray, J. W.: The behavior of scavenging isotopes in marine anoxic environments: lead-210 and polonium-210 in the water column of the Black Sea, *Geochim. Cosmochim. Ac.*, 58, 1795–1811, 1994.
- Wei, C.-L., Chou, L.-H., Tsai, J.-R., Wen, L.-S., and Pai, S.-C.: Comparative geochemistry of ^{234}Th , ^{210}Pb , and ^{210}Po : a case study in the Hung-Tsai Trough off southwestern Taiwan, *Terr. Atmos. Ocean. Sci.*, 20, 411–423, 2009.
- Wei, C.-L., Lin, S.-Y., Sheu, D. D.-D., Chou, W.-C., Yi, M.-C., Santschi, P. H., and Wen, L.-S.: Particle-reactive radionuclides (^{234}Th , ^{210}Pb , ^{210}Po) as tracers for the estimation of export

Wei, C.-L., Lin, S.-Y., Wen, L.-S., and Sheu, D. D.: Geochemical behavior of ^{210}Pb and ^{210}Po in the nearshore waters off western Taiwan, *Mar. Pollut. Bull.*, 64, 214–220, 2012.

5 Wei, C.-L., Chen, P.-R., Lin, S.-Y., Sheu, D. D., Wen, L.-S., and Chou, W.-C.: Distributions of ^{210}Pb and ^{210}Po in surface waters surrounding Taiwan: a synoptic observation, *Deep-Sea Res. Pt. II*, in press, doi:10.1016/j.dsr2.2014.04.010, 2014.

10 Wong, K. M., Jokela, T. A., Eagle, R. J., Brunk, J. L., and Noshkin, V. E.: Radionuclide concentrations, fluxes, and residence times at Santa Monica and San Pedro Basins, *Prog. Oceanogr.*, 30, 353–391, 1992.

Xu, L. Q., Liu, X. D., Sun, L. G., Yana, H., Liu, Y., Luo, Y. H., Huang, J., and Wang, Y. H.: Distribution of radionuclides in the guano sediments of Xisha Islands, South China Sea and its implication, *J. Environ. Radioactiv.*, 101, 362–368, 2010.

15 Yang, W., Huang, Y., Chen, M., Zhang, L., Li, H., Liu, G., and Qiu, Y.: Disequilibria between ^{210}Po and ^{210}Pb in surface waters of the southern South China Sea and their implications, *Sci. China Ser. D*, 49, 103–112, 2006.

Seasonal
distributions and
fluxes of ^{210}Pb and
 ^{210}Po in the Northern
South China Sea

C.-L. Wei et al.

[Title Page](#)
[Abstract](#) [Introduction](#)
[Conclusions](#) [References](#)
[Tables](#) [Figures](#)
[◀](#) [▶](#)
[◀](#) [▶](#)
[Back](#) [Close](#)
[Full Screen / Esc](#)

[Printer-friendly Version](#)
[Interactive Discussion](#)



Seasonal distributions and fluxes of ^{210}Pb and ^{210}Po in the Northern South China Sea

C.-L. Wei et al.

Table 1. Fluxes of total mass (F_{mass}), ^{210}Pb ($F_{\text{Pb-210}}$), and ^{210}Po ($F_{\text{Po-210}}$) measured by sediment trap. Standard deviations of radionuclide data are based on propagated counting error (σ).

Time	Depth m	F_{mass} $\text{mg m}^{-2} \text{d}^{-1}$	$F_{\text{Pb-210}}$ $\text{dpm m}^{-2} \text{d}^{-1}$	$F_{\text{Po-210}}$ $\text{dpm m}^{-2} \text{d}^{-1}$
2–18 Jan 2007	718	425	33.1 ± 0.7	19.2 ± 0.9
2–10 Jan 2007	3454	106	41.6 ± 1.1	25.8 ± 0.8
10–18 Jan 2007	3454	187	51.1 ± 2.3	32.4 ± 1.0
12–28 Jul 2007	1000	32	5.5 ± 0.3	7.0 ± 0.8
12–20 Jul 2007	3000	103	37.1 ± 0.9	52.2 ± 1.6
20–28 Jul 2007	3000	89	31.5 ± 0.7	42.7 ± 1.2

Seasonal distributions and fluxes of ^{210}Pb and ^{210}Po in the Northern South China Sea

C.-L. Wei et al.

[Title Page](#)

[Abstract](#)

[Introduction](#)

[Conclusions](#)

[References](#)

[Tables](#)

[Figures](#)

[◀](#)

[▶](#)

[◀](#)

[▶](#)

[Back](#)

[Close](#)

[Full Screen / Esc](#)

[Printer-friendly Version](#)

[Interactive Discussion](#)

Cruise	Time	$\sum \text{Pb}_d$	$\sum \text{Pb}_p$	$\sum \text{Po}_d$	$\sum \text{Po}_p$	$\sum (\text{Ra} - \text{Pb}_t)$	$\sum (\text{Pb}_t - \text{Po}_t)$
$\times 10^3 \text{ dpm m}^{-2}$							
0–1000 m							
ORI-821	Jan 2007	76.2	8.5	44.1	26.4	62.1	17.5
ORIII-1239	Jul 2007	72.7	7.1	55.5	11.4	51.2	12.9
ORI-845	Oct 2007	67.2	18.1	47.8	9.8	44.6	27.6
ORI-866	May 2008	87.9	15.5	51.9	15.3	35.3	36.2
	Av.	76.0	12.3	49.8	15.8	48.3	23.5
	Sdv.	8.8	5.3	4.9	7.5	11.3	10.4
0–2000 m							
ORIII-1239	Jul 2007	166.8	14.3	103.9	33.5	184.2	43.8
ORI-845	Oct 2007	148.2	38.9	101.3	29.7	181.5	56.1
ORI-866	May 2008	187.5	31.2	107.9	40.3	153.5	70.4
	Av.	167.5	28.1	104.4	34.5	173.1	56.8
	Sdv.	19.6	12.6	3.3	5.4	17.0	13.3
0–3000 m							
ORIII-1239	Jul 2007	269.6	22.7	154.3	63.5	325.9	74.5
ORI-845	Oct 2007	227.2	62.1	157.3	49.0	331.1	83.0
ORI-866	May 2008	304.9	50.6	179.0	71.8	269.3	104.8
	Av.	267.2	45.1	163.5	61.4	308.7	87.4
	Sdv.	38.9	20.3	13.5	11.6	34.3	15.6
0–3500 m							
ORIII-1239	Jul 2007	317.2	29.5	178.3	85.1	398.1	83.3
ORI-845	Oct 2007	266.3	70.1	184.8	58.0	409.8	93.6
ORI-866	May 2008	351.2	69.0	201.8	95.1	330.0	123.3
	Av.	311.6	56.2	188.3	79.4	379.3	100.1
	Sdv.	42.7	23.2	12.1	19.2	43.1	20.8

Table A1. Depth, total suspended matter (TSM) concentration, dissolved ($^{210}\text{Pb}_d$) and particulate ($^{210}\text{Pb}_p$) ^{210}Pb , and dissolved ($^{210}\text{Po}_d$) and particulate ($^{210}\text{Po}_p$) ^{210}Po measured from different cruises to the SEATS station. Standard deviations of radionuclide data are based on counting error (1σ).

Cruise	Depth	TSM	$^{210}\text{Pb}_d$	$^{210}\text{Pb}_p$	$^{210}\text{Po}_d$	$^{210}\text{Po}_p$
			m	mg L ⁻¹	dpm (100 L) ⁻¹	
ORI-821 Jan 2007	0	0.18	7.36 ± 0.51	2.06 ± 0.24	2.12 ± 0.20	1.40 ± 0.19
	5	0.32	9.43 ± 0.68	0.89 ± 0.15	2.55 ± 0.27	1.17 ± 0.19
	10	0.20	6.83 ± 0.50	0.63 ± 0.11	3.27 ± 0.37	1.87 ± 0.33
	20	0.13	7.01 ± 0.49	0.56 ± 0.11	1.78 ± 0.25	1.49 ± 0.22
	30	0.30	7.55 ± 0.58	0.73 ± 0.16	2.96 ± 0.35	1.43 ± 0.26
	40	0.27	7.20 ± 0.48	1.18 ± 0.16	3.20 ± 0.36	1.50 ± 0.25
	50	1.11	8.34 ± 0.64	0.88 ± 0.17	2.77 ± 0.33	4.81 ± 0.48
	60	0.17	8.06 ± 0.65	0.78 ± 0.15	3.83 ± 0.42	1.72 ± 0.25
	100	0.13	6.71 ± 0.49	1.56 ± 0.15	4.04 ± 0.38	4.89 ± 0.41
	160	0.19	8.37 ± 0.66	1.17 ± 0.14	7.61 ± 0.56	5.90 ± 0.57
	225	0.34	8.90 ± 0.58	1.24 ± 0.14	5.74 ± 0.47	1.70 ± 0.28
	300	0.10	6.54 ± 0.42	0.72 ± 0.11	5.87 ± 0.44	2.82 ± 0.37
	500	0.18	8.25 ± 0.53	0.50 ± 0.12	4.12 ± 0.39	1.42 ± 0.23
ORIII-1239 Jul 2007	700	0.15	8.15 ± 0.55	0.44 ± 0.07	3.30 ± 0.34	3.12 ± 0.36
	850	0.10	6.10 ± 0.47	1.11 ± 0.11	3.93 ± 0.39	2.57 ± 0.32
	1000	0.11	8.43 ± 0.64	1.33 ± 0.12	3.88 ± 0.38	1.98 ± 0.24
	0	0.19	7.59 ± 0.54	0.60 ± 0.10	2.60 ± 0.24	0.51 ± 0.10
	5	0.23	5.96 ± 0.62	0.32 ± 0.09	2.71 ± 0.32	0.88 ± 0.27
	10	0.51	7.82 ± 0.65	0.42 ± 0.11	2.23 ± 0.33	1.06 ± 0.26
	20	0.25	7.63 ± 0.49	0.33 ± 0.07	2.19 ± 0.36	0.63 ± 0.21
	30	0.28	5.77 ± 0.71	0.50 ± 0.10	2.09 ± 0.27	0.87 ± 0.28
	50	0.21	6.65 ± 0.73	0.59 ± 0.11	2.62 ± 0.38	0.61 ± 0.22
	75	0.18	8.34 ± 0.79	0.32 ± 0.10	4.58 ± 0.53	0.90 ± 0.27
	100	0.12	6.29 ± 0.50	0.26 ± 0.06	7.16 ± 0.68	0.41 ± 0.15
	160	0.19	8.15 ± 0.79	0.60 ± 0.15	7.02 ± 0.66	0.57 ± 0.20
	250	0.30	6.62 ± 0.66	0.45 ± 0.14	9.60 ± 0.85	0.87 ± 0.16
	300	0.15	7.65 ± 0.68	0.86 ± 0.17	8.25 ± 0.72	0.98 ± 0.26
	400	0.46	6.90 ± 0.57	0.81 ± 0.11	5.91 ± 0.57	1.51 ± 0.20
	500	0.31	9.29 ± 0.73	0.73 ± 0.14	5.24 ± 0.67	0.95 ± 0.27
	600	0.20	6.39 ± 0.58	0.77 ± 0.16	5.50 ± 0.46	1.06 ± 0.27
	800	0.42	6.80 ± 0.61	0.79 ± 0.13	3.40 ± 0.29	1.41 ± 0.30
	1000	0.30	7.87 ± 0.78	0.91 ± 0.15	5.43 ± 0.47	1.94 ± 0.35
	1500	0.28	9.55 ± 0.78	0.75 ± 0.16	4.48 ± 0.45	2.21 ± 0.44
	2000	0.23	10.68 ± 0.97	0.48 ± 0.12	4.99 ± 0.50	2.45 ± 0.44
	2500	0.26	9.98 ± 0.94	0.87 ± 0.16	4.79 ± 0.45	3.14 ± 0.49
	3000	0.27	10.48 ± 0.75	1.12 ± 0.14	5.58 ± 0.38	3.26 ± 0.39
	3500	0.33	8.58 ± 0.42	1.59 ± 0.16	4.03 ± 0.37	5.41 ± 0.59

Table A1. Continued.

Cruise	Depth	TSM mg L ⁻¹	²¹⁰ Pb _d	²¹⁰ Pb _p	²¹⁰ Po _d	²¹⁰ Po _p
			dpm (100 L) ⁻¹			
ORI-845 Oct 2007	0	0.26	6.68 ± 0.32	0.70 ± 0.12	2.83 ± 0.23	0.56 ± 0.08
	5	0.36	6.91 ± 0.30	0.64 ± 0.08	2.67 ± 0.26	0.77 ± 0.13
	10	0.56	2.55 ± 0.16	0.89 ± 0.11	2.67 ± 0.31	0.61 ± 0.11
	20	0.18	8.76 ± 0.28	0.57 ± 0.06	3.01 ± 0.28	0.60 ± 0.12
	40	0.31	4.38 ± 0.23	0.58 ± 0.07	2.37 ± 0.31	0.94 ± 0.16
	50	0.32	5.15 ± 0.24	0.50 ± 0.07	2.60 ± 0.30	0.63 ± 0.13
	60	0.27	5.43 ± 0.21	0.69 ± 0.08	4.04 ± 0.31	0.54 ± 0.10
	80	0.28	5.66 ± 0.24	1.02 ± 0.08	5.01 ± 0.44	0.07 ± 0.04
	100	0.23	2.60 ± 0.16	0.94 ± 0.10	3.84 ± 0.36	0.28 ± 0.09
	150	0.31	3.46 ± 0.21	3.30 ± 0.24	7.37 ± 0.45	0.97 ± 0.11
	200	0.20	7.49 ± 0.36	1.35 ± 0.11	5.79 ± 0.52	0.74 ± 0.13
	300	0.18	5.62 ± 0.22	2.49 ± 0.19	4.90 ± 0.41	1.08 ± 0.15
	500	0.21	7.76 ± 0.46	1.53 ± 0.18	5.13 ± 0.33	0.84 ± 0.13
	1000	0.23	7.27 ± 0.26	2.14 ± 0.12	4.03 ± 0.33	1.46 ± 0.21
	1500	0.34	8.61 ± 0.40	1.83 ± 0.16	5.70 ± 0.45	2.21 ± 0.30
	2000	0.28	7.94 ± 0.27	2.55 ± 0.32	5.97 ± 0.41	2.08 ± 0.19
	2500	0.22	7.79 ± 0.60	2.00 ± 0.14	6.15 ± 0.52	1.56 ± 0.19
	3000	0.19	8.05 ± 0.33	2.71 ± 0.14	4.10 ± 0.40	2.48 ± 0.25
	3500	0.09	7.61 ± 0.41	0.51 ± 0.07	6.90 ± 0.39	1.14 ± 0.18
ORI-866 May 2008	0	0.41	9.19 ± 0.38	0.74 ± 0.09	4.78 ± 0.31	1.39 ± 0.19
	10	0.16	10.07 ± 0.62	1.26 ± 0.18	3.95 ± 0.33	1.59 ± 0.19
	30	0.38	9.41 ± 0.59	0.52 ± 0.07	3.53 ± 0.29	1.20 ± 0.18
	50	0.39	9.62 ± 0.57	1.04 ± 0.16	5.33 ± 0.35	1.50 ± 0.17
	75	0.23	8.91 ± 0.47	1.46 ± 0.18	5.58 ± 0.40	1.25 ± 0.17
	100	0.32	10.50 ± 0.57	0.61 ± 0.08	5.27 ± 0.36	1.02 ± 0.17
	120	0.39	11.80 ± 0.65	0.74 ± 0.07	6.13 ± 0.41	1.24 ± 0.16
	160	0.25	9.59 ± 0.53	0.80 ± 0.07	7.21 ± 0.46	1.15 ± 0.17
	200	0.21	10.70 ± 0.56	0.83 ± 0.10	5.89 ± 0.36	1.29 ± 0.18
	250	0.20	10.70 ± 0.40	0.93 ± 0.10	7.45 ± 0.46	1.23 ± 0.16
	300	0.54	8.20 ± 0.33	1.47 ± 0.21	5.83 ± 0.39	1.35 ± 0.19
	400	0.41	8.97 ± 0.34	2.45 ± 0.30	4.05 ± 0.34	1.69 ± 0.18
	600	0.38	6.86 ± 0.43	1.14 ± 0.15	4.74 ± 0.35	1.16 ± 0.18
	800	0.27	9.17 ± 0.34	2.24 ± 0.31	5.60 ± 0.42	1.84 ± 0.18
	1000	0.15	8.11 ± 0.38	1.53 ± 0.15	4.36 ± 0.34	2.29 ± 0.24
	2000	0.27	11.80 ± 0.40	1.60 ± 0.20	6.83 ± 0.41	2.71 ± 0.26
	2500	0.18	12.55 ± 0.44	1.42 ± 0.21	7.85 ± 0.34	3.19 ± 0.32
	3000	0.24	10.06 ± 0.54	3.34 ± 0.38	5.91 ± 0.27	3.49 ± 0.28
	3500	0.16	8.44 ± 0.38	4.01 ± 0.19	3.22 ± 0.25	5.85 ± 0.42
	3700	0.20	4.33 ± 0.22	5.59 ± 0.29	1.85 ± 0.17	5.18 ± 0.40

[Title Page](#)[Abstract](#)[Introduction](#)[Conclusions](#)[References](#)[Tables](#)[Figures](#)[◀](#)[▶](#)[◀](#)[▶](#)[Back](#)[Close](#)[Full Screen / Esc](#)[Printer-friendly Version](#)[Interactive Discussion](#)

Seasonal distributions and fluxes of ^{210}Pb and ^{210}Po in the Northern South China Sea

C.-L. Wei et al.

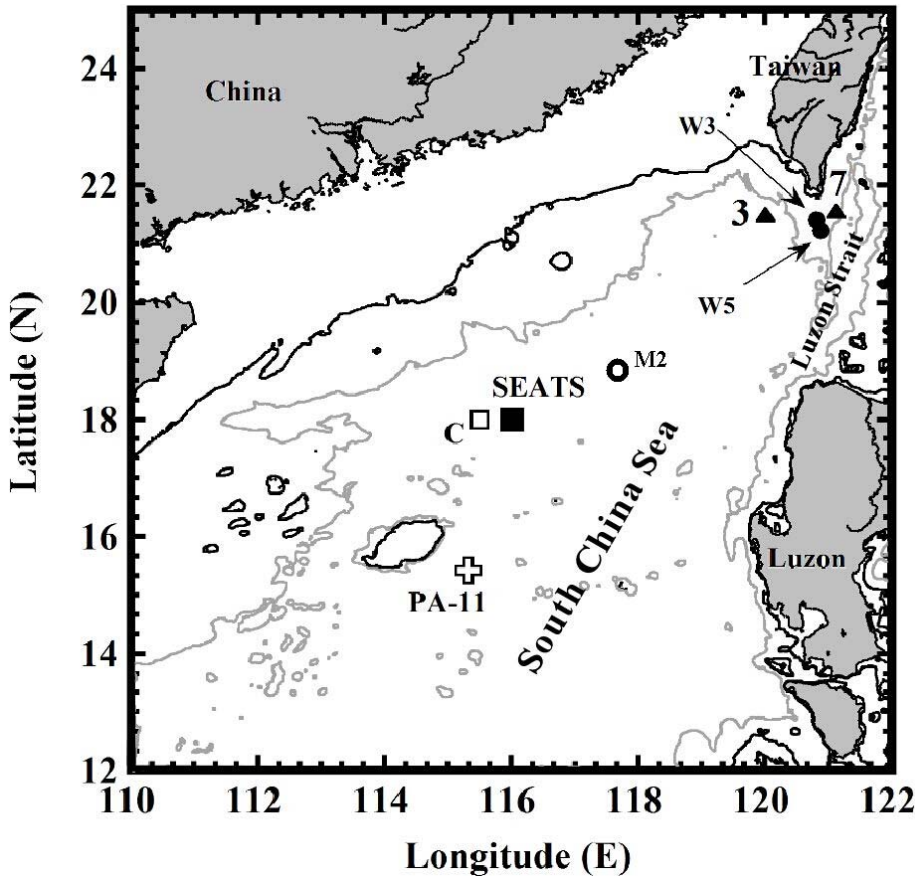


Figure 1. Location of the SEATS station and sites of previous studies in the South China Sea. Bathymetry contours of 200 m and 2000 m are shown as black and gray lines, respectively. Stations of previous studies are: M2 of Chung et al. (2004), PA-11 of Obata et al. (2004), C, W3, W5 of Chung and Wu (2005), 3, 7 of Chen and Chung (1997).

11560

Seasonal distributions and fluxes of ^{210}Pb and ^{210}Po in the Northern South China Sea

C.-L. Wei et al.

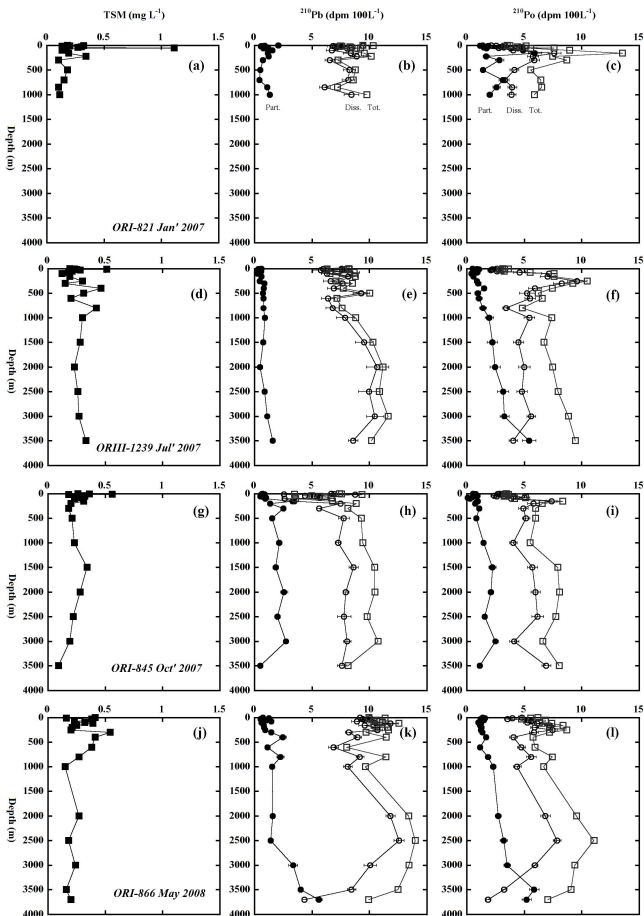


Figure 2. Vertical profiles of TSM concentration, $^{210}\text{Pb}_t$, $^{210}\text{Pb}_d$, $^{210}\text{Pb}_p$, $^{210}\text{Po}_t$, $^{210}\text{Po}_d$ and $^{210}\text{Po}_p$ measured from **(a–c)** ORI-821, **(d–f)** ORIII-1239, **(g–i)** ORI-845, and **(j–l)** ORI-866. Error bars represent uncertainty estimated by counting statistics of radionuclide data ($\pm 1\sigma$).

Seasonal distributions and fluxes of ^{210}Pb and ^{210}Po in the Northern South China Sea

C.-L. Wei et al.

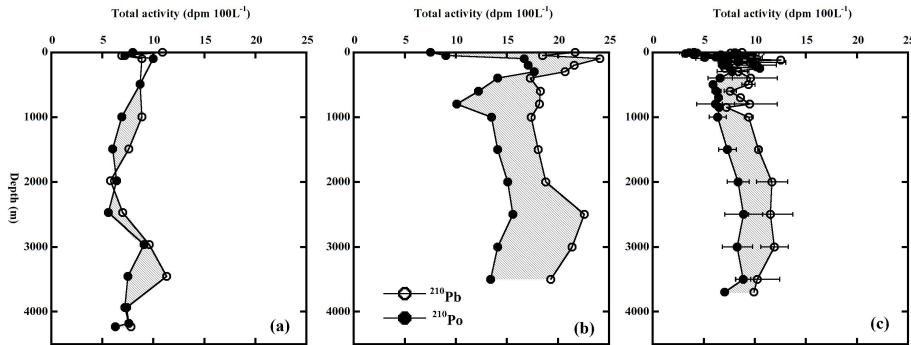


Figure 3. Vertical profiles of $^{210}\text{Pb}_t$ and $^{210}\text{Po}_t$ plotted from (a) the data reported at station PA-11 of Obata et al. (2004), (b) the average values of the two profiles at station C of Chung and Wu (2005), and (c) the average values with standard deviations measured by the four cruises of this study. Shaded area represents deficiency of ^{210}Pb relative to ^{210}Po .

[Title Page](#) | [Abstract](#) | [Introduction](#)
[Conclusions](#) | [References](#)
[Tables](#) | [Figures](#)
[◀](#) | [▶](#)
[◀](#) | [▶](#)
[Back](#) | [Close](#)
[Full Screen / Esc](#)

[Printer-friendly Version](#)
[Interactive Discussion](#)

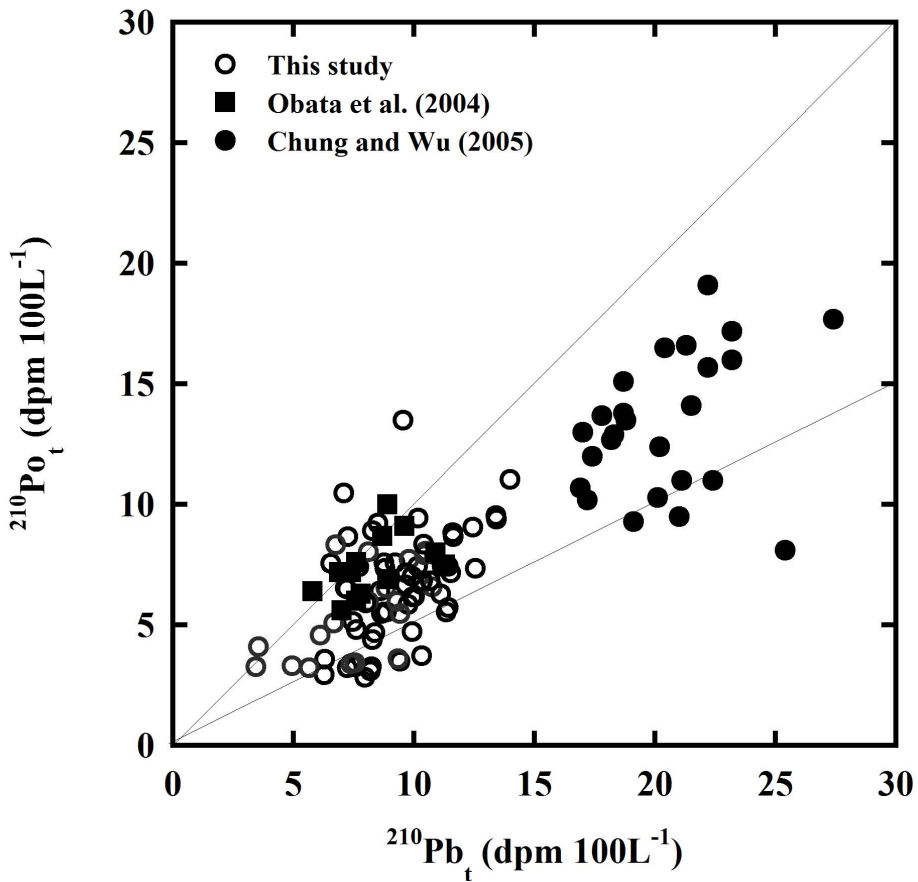


Figure 4. Correlation of $^{210}\text{Pb}_t$ and $^{210}\text{Po}_t$ for the data at station PA-11 of Obata et al. (2004) (solid square), at station C of Chung and Wu (2005) (solid circle), and at station SEATS of this study (open circle). Slopes of 0.5 and 1 are shown as solid lines.

Seasonal distributions and fluxes of ^{210}Pb and ^{210}Po in the Northern South China Sea

C.-L. Wei et al.

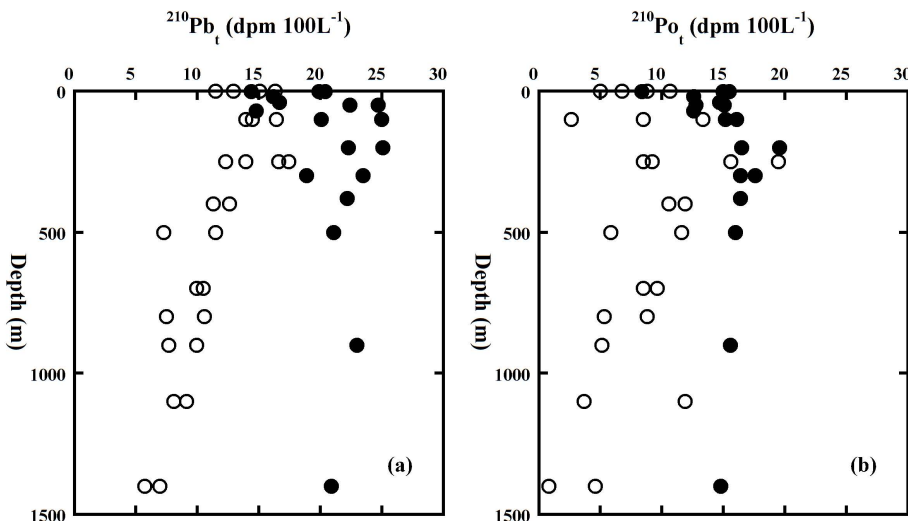


Figure 5. Vertical profiles of $^{210}\text{Pb}_t$ and $^{210}\text{Po}_t$ redrawn from stations 3 and 7 of Chen and Chung (1997) (open circle) and stations W3 and W5 of Chung and Wu (2005) (solid circle).

Title Page

Abstract

Introduction

Conclusion

References

Tables

Figures

1

1

Back

Close

Full Screen / Esc

• 100 •

Seasonal distributions and fluxes of ^{210}Pb and ^{210}Po in the Northern South China Sea

C.-L. Wei et al.

Title Page

Abstract

Introduction

Conclusions

References

Tables

Figures

1

1

◀

1

Back

Close

Full Screen / Esc

Interactive Discussion

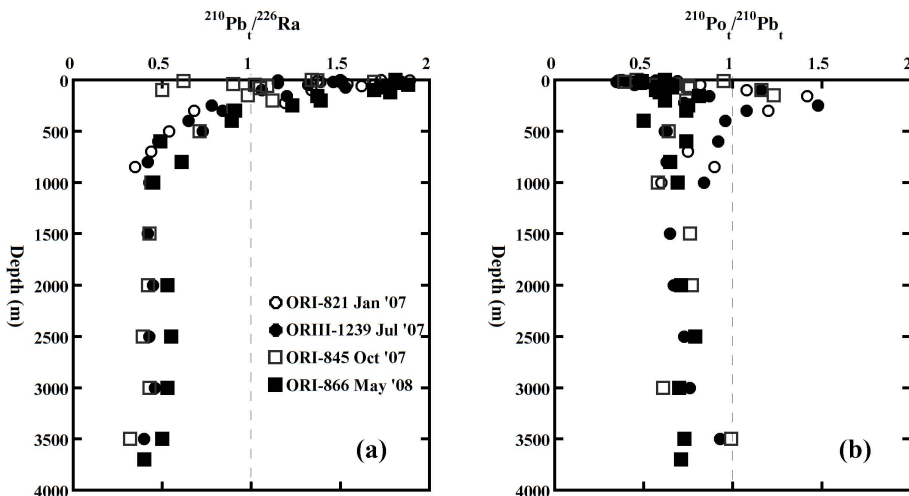


Figure 6. Vertical profiles of (a) $^{210}\text{Pb}_t/^{226}\text{Ra}$ ratio and (b) $^{210}\text{Po}_t/^{210}\text{Pb}_t$ ratio of the four cruises to the SEATS station. Dashed line at unity indicates the secular equilibrium between daughter and parent radionuclides.

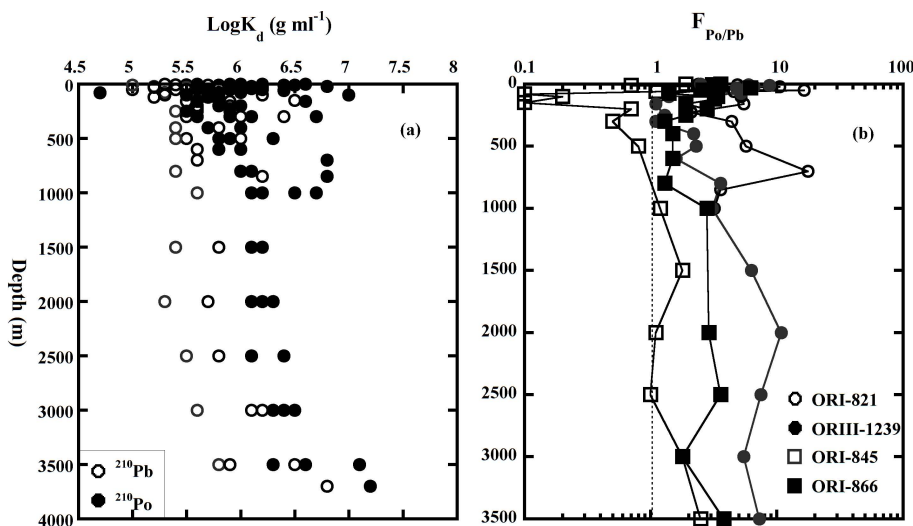


Figure 7. Vertical profiles of (a) $K_d(\text{Pb})$ and $K_d(\text{Po})$ and (b) fractionation factor of ^{210}Po and ^{210}Pb . Dashed line at unity indicates the same partitioning of dissolved and particulate phases for ^{210}Po and ^{210}Pb .

Seasonal distributions and fluxes of ^{210}Pb and ^{210}Po in the Northern South China Sea

C.-L. Wei et al.

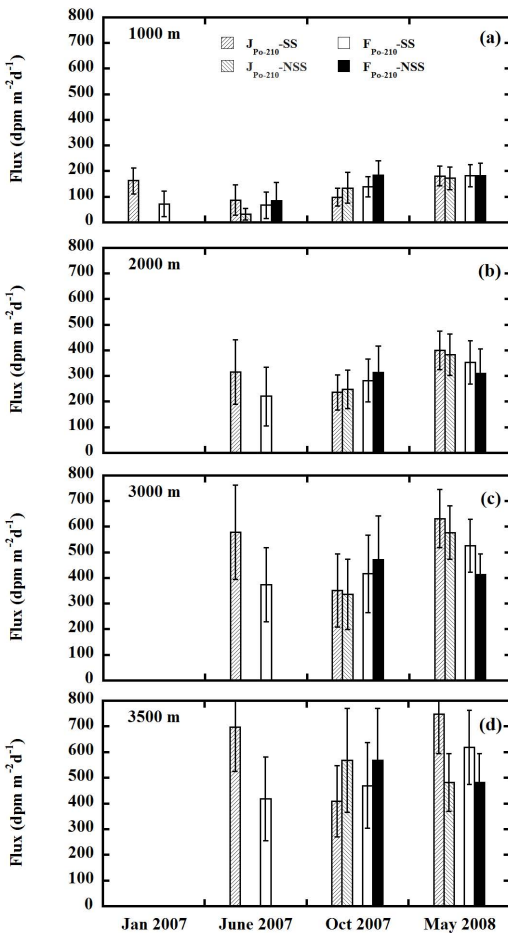


Figure 8. Scavenging ($J_{\text{Po-210}}$) and removal ($F_{\text{Po-210}}$) fluxes of ^{210}Po calculated by steady-state (SS) and non-steady-state (NSS) models at (a) 1000 m, (b) 2000 m, (c) 3000 m, and (d) 3500 m.